Brans-Dicke scalar field cosmological model in Lyra's geometry

Dinesh Chandra Maurya[1,*] and Rashid Zia[2,†]

[1]*Department of Mathematics, Faculty of Engineering & Technology, IASE (Deemed to be University), Sardarshahar-331 403 Rajsthan, India*

[2]*Department of Mathematics, BBS College of Engineering and Technology, Allahabad, UP 211003, India*

(Received 22 December 2017; published 8 July 2019)

In this paper, we have developed a new cosmological model in Einstein's modified gravity theory using two types of modification: (i) Geometrical modification, in which we have used Lyra's geometry in the left-hand side of the Einstein field equations (EFE), and (ii) modification in gravity (energy momentum tensor) on the right-hand side of EFE, as per the Brans-Dicke (BD) model. With these two modifications, we have investigated spatially homogeneous and anisotropic Bianchi type-I cosmological models of Einstein's Brans-Dicke theory of gravitation in Lyra geometry. The model represents an accelerating universe at present and a decelerating in the past and is considered to be dominated by dark energy. Gauge function β and BD-scalar field ϕ are considered as a candidate for the dark energy and is responsible for the present acceleration. The derived model agrees at par with the recent supernovae (SN Ia) observations. We have set BD-coupling constant ω to be greater than 40000, seeing the solar system tests and evidence. We have discussed the various physical and geometrical properties of the models and have compared them with the corresponding relativistic models.

DOI: 10.1103/PhysRevD.100.023503

I. INTRODUCTION

Einstein formulated the theory of general relativity (GR) in 1915, in which he described gravity as a geometrical property of space and time. In particular, the curvature of spacetime was proposed to be directly related to the energy and momentum of whatever matter and radiation are present in the universe. The relation was specified by the Einstein field equations (EFE), which are a system of partial differential equations. The original EFE were written in the form $R_{\mu\nu} - \frac{1}{2} R g_{\mu\nu} = \frac{8\pi G}{c^4} T_{\mu\nu}$, where $R_{\mu\nu}$ is Ricci curvature tensor, R is the scalar curvature, $g_{\mu\nu}$ is the metric tensor, and $T_{\mu\nu}$ is the energy momentum tensor.

EFE are a foundation on which various cosmological models have been constructed. Soon after the formulation of the field equation, Einstein applied these equations for constructing the model of the universe. Einstein's original field equations support an expanding universe. But at that time, it was believed that the universe is static. So to make his model static, Einstein modified his original EFE by introducing a positive constant Λ in his field equations and termed this as a cosmological constant. But, after Hubble's discovery in 1929, it was established that the universe is not static but expanding. So, under the new scenario, Einstein abandoned the cosmological constant, calling it the "biggest blunder" of his life, and returned to his original field equations. Inspired by geometrizing gravitation, in 1918 Weyl [1] proposed a more general theory in which both gravitation and electromagnetism are described geometrically.

So, to accommodate new findings or for the sake of generalization, various modifications have been proposed by researchers in original EFE from time to time, since its inception. Some researchers modified the geometrical part, whereas some proposed the modification in the energy momentum part of the EFE.

In the present paper, we have applied both types of modification simultaneously. On the left-hand side, we have used Lyra's geometry (geometrical modification) in EFE; and on the right-hand side, we have modified the energy momentum tensor as per the Brans-Dicke model. The motivation behind such modifications are as follows: In general relativity Einstein succeeded in geometrizing gravitation by identifying the metric tensor with the gravitational potentials. In 1951, Lyra proposed a modification of Riemannian geometry by introducing a gauge function into the structureless manifold [2] (see also [3]). Based on Lyra geometry, a new scalar-tensor theory of gravitation which was an analogue of the Einstein field equations was proposed by Sen and Dunn [4,5]. An interesting feature of this model is that it keeps the spirit of Einstein's principle of geometrization, since both the scalar and tensor fields have more or less intrinsic geometrical significance. In contrast, in the Brans-Dicke theory, the tensor field alone is geometrized and the scalar field remains alien to the

*dcmaurya563@gmail.com
†rashidzya@gmail.com

geometry [6,7]. By incorporating both of these separate modifications into a single theory, we have arrived at a more general method of geometrizing gravitation.

Also, in the construction of recent cosmological models, two problems prevail: The late time acceleration problem, and the existence of big-bang singularity. To deal with the first problem, one of the ways is by introducing the gauge function into the structureless manifold in the framework of Lyra geometry. In this approach, the cosmological constant of EFE naturally arises from the geometry, instead of introducing it in an *ad hoc* way. In fact, the constant displacement vector field plays the role of cosmological constant which can be responsible for the late-time cosmological acceleration of the universe [8,9]. For the second problem, recently a new mechanism for avoiding the big-bang singularity was proposed in the framework of the emergent universe scenario (see [10–12]). The emergent universe scenario is a past-eternal inflationary model in which the horizon problem is solved before the beginning of inflation and the big-bang singularity is removed.

To date, various researchers have studied cosmology in Lyra's geometry (see [8,9,13–29]) with both a constant displacement field and a time-dependent one. For instance, in [20] the displacement field is allowed to be time dependent, and the Friedmann-Robertson-Walker (FRW) models are derived in Lyra's manifold. Those models are free of the big-bang singularity and solve the entropy and horizon problems which beset the standard models based on Riemannian geometry. Recently, cosmological models in the framework of Lyra's geometry in different contexts are investigated in several papers (see [21–29]).

Also, in the past few decades, there has been considerable interest in alternative theories of gravitation coursed by the investigations of inflation and, especially, late cosmological acceleration which is well proved in many papers (see [30–35]). In order to explain such unexpected behavior of our universe, one can modify the gravitational theory (see [36–41]), or construct various field models of the so-called dark energy (DE), for which equation of state (EoS) satisfies $\gamma = \frac{p}{\rho} < -\frac{1}{3}$ (see [42–48]). Presently, there is an uprise of interest in scalar fields in GR and alternative theories of gravitation in this context. Therefore, the study of cosmological scalar-field models in Lyra's geometry is relevant for the cosmic acceleration models. A Bianchi type-I dust filled accelerating Brans-Dicke cosmological model with cosmological constant Λ as a dark energy candidate was investigated by Goswami *et al.* [49], and Brans-Dicke scalar-field cosmological models in Lyra geometry with a time-dependent deceleration parameter was studied by [50]. Recently, a detailed review on dark energy/modified gravity problem was presented by [51].

Most studies in Lyra's cosmology involve a perfect fluid. Strangely, at least to our knowledge, the case of the scalar field in Lyra's cosmology was not studied properly. Here we would like to fill this gap. In this paper, we will consider a scalar field Brans-Dicke cosmology in the context of Lyra's geometry. With motivation provided above, we have investigated Einstein's modified field equations for the spatially homogeneous anisotropic Bianchi type-I spacetime metric within the framework of Lyra's geometry.

The outline of the paper is as follows: Section I is introductory in nature. In Sec. II, the field equations in Lyra geometry with Brans-Dicke modifications are described. Section III deals with the cosmological solutions that have established relations among energy parameters Ω_m, Ω_σ, and Ω_β. In Sec. IV, we obtained expressions for Hubble's constant, luminosity distance, and apparent magnitude in terms of redshift and scale factor. We have also estimated the present values of energy parameters and Hubble's constant. The deceleration parameter (DP), age of the universe, and certain physical properties of the universe are presented in Sec. V. The discussion of results are given in Sec. VI. Finally, conclusions are summarized in Sec. VII.

II. LYRA GEOMETRY AND EINSTEIN'S BRANS-DICKE FIELD EQUATIONS

Lyra geometry is a modification of Riemannian geometry by introducing a gauge function into the structureless manifold [2]; see also [3]. Lyra defined a displacement vector between two neighboring points $P(x^\mu)$ and $Q(x^\mu + dx^\mu)$ as Adx^μ where $A = A(x^\mu)$ is a nonzero gauge function of the coordinates. The gauge function $A(x^\mu)$ together with the coordinate system x^μ form a reference system (A, x^μ). The transformation to a new reference system $(\bar{A}, \bar{x}^\mu)$ is given by the following functions:

$$\bar{A} = \bar{A}(A, x^\mu), \qquad \bar{x}^\mu = \bar{x}(x^\mu), \tag{1}$$

where $\frac{\partial \bar{A}}{\partial A} \neq 0$ and $\det(\frac{\partial \bar{x}}{\partial x}) \neq 0$.

The symmetric affine connections $\tilde{\Gamma}^\mu_{\nu\sigma}$ on this manifold are given by

$$\tilde{\Gamma}^\mu_{\nu\sigma} = \frac{1}{A}\Gamma^\mu_{\nu\sigma} + \frac{1}{2}(\delta^\mu_\nu \psi_\sigma + \delta^\mu_\sigma \psi_\nu - g_{\nu\sigma}\psi^\mu), \tag{2}$$

where the connection $\Gamma^\mu_{\nu\sigma}$ is defined in terms of the metric tensor $g_{\mu\nu}$ as in Riemannian geometry and $\psi^\mu = g^{\mu\nu}\psi_\nu$ is the so-called displacement vector field of Lyra geometry. It is shown by Lyra [2], and also by Sen [4], that in any general reference system, the displacement vector field ψ^μ arises as a natural consequence of the formal introduction of the gauge function $A(x^\mu)$ into the structureless manifold. Equation (2) shows that the component of the affine connection depends not only on metric $g_{\mu\nu}$ but also on the displacement vector field ψ^μ. The line element (metric) in Lyra geometry is given by

$$ds^2 = A^2 g_{\mu\nu} dx^\mu dx^\nu, \tag{3}$$

which is invariant under both of the coordinate and gauge transformations. The infinitesimal parallel transport of a vector field V^μ is given by

$$\delta V^\mu = \hat{\Gamma}^\mu_{\nu\sigma} V^\nu A dx^\sigma, \tag{4}$$

where $\hat{\Gamma}^\mu_{\nu\sigma} = \tilde{\Gamma}^\mu_{\nu\sigma} - \frac{1}{2}\delta^\mu_\nu \psi_\sigma$ which is not symmetric with respect to ν and σ. In Lyra geometry, unlike Weyl geometry, the connection is metric preserving as in Riemannian geometry which indicates that length transfers are integrable. This means that the length of a vector is conserved upon parallel transports, as in Riemannian geometry.

The curvature tensor of Lyra geometry is defined in the same manner as in Riemannian geometry and is given by

$$\tilde{R}^\mu_{\nu\rho\sigma} = A^{-2}\left[\frac{\partial}{\partial x^\rho}(A\hat{\Gamma}^\mu_{\nu\sigma}) - \frac{\partial}{\partial x^\sigma}(A\hat{\Gamma}^\mu_{\nu\rho}) + A^2(\hat{\Gamma}^\mu_{\lambda\rho}\hat{\Gamma}^\lambda_{\nu\sigma} - \hat{\Gamma}^\mu_{\lambda\sigma}\hat{\Gamma}^\lambda_{\nu\rho})\right]. \tag{5}$$

Then, the curvature scalar of Lyra geometry will be

$$\tilde{R} = A^{-2}R + 3A^{-1}\nabla_\mu\psi^\mu + \frac{3}{2}\psi^\mu\psi_\mu + 2A^{-1}(\log A^2)_{,\mu}\psi^\mu, \tag{6}$$

where R is the Riemannian curvature scalar and the covariant derivative is taken with respect to the Christoffel symbols of the Riemannian geometry.

The invariant volume integral in the four-dimensional Lyra manifold is given by

$$I = \int \sqrt{-g} L (A dx)^4, \tag{7}$$

where L is an invariant scalar in this geometry. Using the normal gauge $A = 1$ and $L = \tilde{R}$ through the equations (6) and (7) results in

$$\tilde{R} = R + 3\nabla_\mu\psi^\mu + \frac{3}{2}\psi^\mu\psi_\mu, \tag{8}$$

$$I = \int \sqrt{-g}\tilde{R} dx^4. \tag{9}$$

Therefore the Lagrangian for the Brans-Dicke theory in Lyra geometry can be defined as

$$\tilde{L}_{\mathrm{BDT}} = \phi\left(\tilde{R} - w\frac{\phi_{,\mu}\phi^{,\mu}}{\phi^2}\right) + 16\pi L_{\mathrm{mat}}, \tag{10}$$

where $\tilde{R} = R + 3\nabla_\mu\psi^\mu + \frac{3}{2}\psi^\mu\psi_\mu$ is the curvature scalar of Lyra geometry [2] using normal gauge transformations, ψ^μ is a displacement vector field of Lyra geometry, R is curvature scalar in Riemannian geometry, w is the Brans-Dicke coupling constant, ϕ is the Brans-Dicke scalar field as mentioned in the first section, and L_{mat} is Lagrangian for matter. Therefore, the action for this Lagrangian is defined as

$$I = \int\left[\phi\left(R + 3\nabla_\mu\psi^\mu + \frac{3}{2}\psi^\mu\psi_\mu - w\frac{\phi_{,\mu}\phi^{,\mu}}{\phi^2}\right) + 16\pi L_{\mathrm{mat}}\right]\sqrt{-g}d^4x. \tag{11}$$

By varying the action I of the gravitational field with respect to the metric tensor components $g^{\mu\nu}$ and ϕ, respectively, we obtained the following Einstein's Brans-Dicke field equations in Lyra geometry:

$$G_{\mu\nu} + \frac{3}{2}\psi_\mu\psi_\nu - \frac{3}{4}g_{\mu\nu}\psi_\sigma\psi^\sigma = -\frac{8\pi T_{\mu\nu}}{\phi c^4} - \frac{w}{\phi^2}\left(\phi_{,\mu}\phi_{,\nu} - \frac{1}{2}g_{\mu\nu}\phi_{,\sigma}\phi^{,\sigma}\right) - \frac{1}{\phi}(\phi_{,\mu,\nu} - g_{\mu\nu}\Box\phi), \tag{12}$$

$$\Box\phi = \phi^{;\mu}_{,\mu} = \frac{8\pi T}{(3+2w)c^2}, \tag{13}$$

where $G_{\mu\nu}$ is the Einstein curvature tensor, $(,)$ and $(\cdot)$ denote the covariant and contravariant derivatives, and other symbols have their usual meanings in Riemannian geometry. The metric in Lyra geometry is defined by $ds^2 = g_{\mu\nu}(Adx^\mu)(Adx^\nu)$, where A is the gauge transformations. Using normal gauge transformation $(A = 1)$ the above metric becomes $ds^2 = g_{\mu\nu}dx^\mu dx^\nu$ as in Riemannian geometry.

We assume a perfect fluid form for the energy-momentum tensor

$$T_{\mu\nu} = (\rho + p)u_\mu u_\nu + p g_{\mu\nu} \tag{14}$$

and comoving coordinates $u_\mu u^\mu = -1$. We also let ψ_μ be the timelike constant vector

$$\psi_\mu = (\beta, 0, 0, 0), \tag{15}$$

where β is a constant. The metric for Bianchi type-I spacetime is given by

$$ds^2 = -dt^2 + A^2dx^2 + B^2dy^2 + C^2dz^2, \tag{16}$$

where A, B, and C are functions of cosmic time t alone.

For the metric (16), solving the field equations (14), we get the following field equations:

$$\frac{\dot{A}\dot{B}}{AB}+\frac{\dot{B}\dot{C}}{BC}+\frac{\dot{A}\dot{C}}{AC}-\frac{3}{4}\beta^2=\frac{8\pi\rho}{\phi c^2}-\frac{w}{2}\left(\frac{\dot{\phi}}{\phi}\right)^2+\frac{\dot{\phi}}{\phi}\left(\frac{\dot{A}}{A}+\frac{\dot{B}}{B}+\frac{\dot{C}}{C}\right), \tag{17}$$

$$\frac{\ddot{B}}{B}+\frac{\ddot{C}}{C}+\frac{\dot{B}\dot{C}}{BC}+\frac{3}{4}\beta^2=-\frac{8\pi p}{\phi c^2}+\frac{w}{2}\left(\frac{\dot{\phi}}{\phi}\right)^2+\frac{\dot{\phi}}{\phi}\left(\frac{\dot{B}}{B}+\frac{\dot{C}}{C}\right)+\frac{\ddot{\phi}}{\phi}, \tag{18}$$

$$\frac{\ddot{A}}{A}+\frac{\ddot{C}}{C}+\frac{\dot{A}\dot{C}}{AC}+\frac{3}{4}\beta^2=-\frac{8\pi p}{\phi c^2}+\frac{w}{2}\left(\frac{\dot{\phi}}{\phi}\right)^2+\frac{\dot{\phi}}{\phi}\left(\frac{\dot{A}}{A}+\frac{\dot{C}}{C}\right)+\frac{\ddot{\phi}}{\phi}, \tag{19}$$

$$\frac{\ddot{A}}{A}+\frac{\ddot{B}}{B}+\frac{\dot{A}\dot{B}}{AB}+\frac{3}{4}\beta^2=-\frac{8\pi p}{\phi c^2}+\frac{w}{2}\left(\frac{\dot{\phi}}{\phi}\right)^2+\frac{\dot{\phi}}{\phi}\left(\frac{\dot{A}}{A}+\frac{\dot{B}}{B}\right)+\frac{\ddot{\phi}}{\phi}, \tag{20}$$

$$\frac{\ddot{\phi}}{\phi}+\frac{\dot{\phi}}{\phi}\left(\frac{\dot{A}}{A}+\frac{\dot{B}}{B}+\frac{\dot{C}}{C}\right)=\frac{8\pi(\rho-3p)}{(2w+3)\phi c^2}. \tag{21}$$

Here overdots denote the derivatives with respect to time t.

III. COSMOLOGICAL SOLUTIONS OF THE FIELD EQUATIONS

The covariant derivative of field equation (12) for Eq. (14), gives the energy conservation law as

$$\dot{\rho}+3H(\rho+p)=0. \tag{22}$$

The equation of state for the model is defined as

$$p=\gamma\rho, \tag{23}$$

where γ is EoS parameter of the fluid filled in the universe and the Hubble parameter H is given by $H=\frac{\dot{a}}{a}$, where a is the average scale factor.

There are two cases for the value of the EoS parameter γ in Eq. (23):

Case I: Taking $\gamma=$ const, integrating Eq. (22), we get

$$\rho=\rho_0(a)^{-3(1+\gamma)}=\rho_0(ABC)^{-(1+\gamma)}. \tag{24}$$

Case II: Taking $\gamma=$ variable and assuming $\gamma=\gamma(a)$ in the form

$$\gamma=\gamma_0+\gamma_a(1-a), \tag{25}$$

where γ_0 is an arbitrary constant and γ_a is the value of $|\frac{d\gamma}{da}|_{a=0}$.

Using this in Eq. (22), we get

$$\rho=a^{-3(1+\gamma_0+\gamma_a)}\exp(\rho_0+3a\gamma_a). \tag{26}$$

In the present model, we will consider case I assuming $\gamma=$ const.

Now, from Eqs. (18)–(20), we obtain

$$\frac{B}{A}=c_2\exp\left(c_1\int\frac{\phi}{a^3}dt\right), \tag{27}$$

$$\frac{C}{A}=c_4\exp\left(c_3\int\frac{\phi}{a^3}dt\right), \tag{28}$$

$$\frac{C}{B}=c_6\exp\left(c_5\int\frac{\phi}{a^3}dt\right). \tag{29}$$

Now, taking the value of arbitrary integrating constants $c_2=c_4=c_6=1$ and $c_1=k, c_3=-k, c_5=-2k$ and assuming

$$D=\exp\left(\int\frac{k\phi}{(ABC)}dt\right), \tag{30}$$

we get the following relations:

$$B=AD \quad \text{and} \quad C=\frac{A}{D}. \tag{31}$$

The average scale factor a is defined as $a=(ABC)^{\frac{1}{3}}$ and using Eq. (31), we obtain

$$a=(ABC)^{\frac{1}{3}}=A. \tag{32}$$

Therefore, from Eqs. (17) to (32), we obtain

$$3\left(\frac{\dot{A}}{A}\right)^2-\left(\frac{\dot{D}}{D}\right)^2-\frac{3}{4}\beta^2=\frac{8\pi\rho}{\phi c^2}-\frac{w}{2}\left(\frac{\dot{\phi}}{\phi}\right)^2+3\frac{\dot{\phi}}{\phi}\left(\frac{\dot{A}}{A}\right), \tag{33}$$

$$2\left(\frac{\ddot{A}}{A}\right)+\left(\frac{\dot{A}}{A}\right)^2+\left(\frac{\dot{D}}{D}\right)^2+\frac{3}{4}\beta^2 =-\frac{8\pi p}{\phi c^2}+\frac{w}{2}\left(\frac{\dot{\phi}}{\phi}\right)^2+2\frac{\dot{\phi}}{\phi}\left(\frac{\dot{A}}{A}\right)+\frac{\ddot{\phi}}{\phi}, \tag{34}$$

$$\frac{d}{dt}\left(\frac{\dot{D}}{D}\right)+\frac{\dot{D}}{D}\left(3\frac{\dot{A}}{A}-\frac{\dot{\phi}}{\phi}\right)=0, \tag{35}$$

$$\frac{\ddot{\phi}}{\phi}+3\frac{\dot{\phi}}{\phi}\left(\frac{\dot{A}}{A}\right)=\frac{8\pi(\rho-3p)}{(2w+3)\phi c^2}, \tag{36}$$

$$\frac{\dot{\rho}}{\rho}+3(1+\gamma)\frac{\dot{A}}{A}=0. \tag{37}$$

From Eq. (31), we get

$$\frac{\dot{D}}{D}\frac{A^3}{\phi} = k \Rightarrow \frac{\dot{D}}{D} = \frac{k\phi}{A^3}. \tag{38}$$

Now, we define the matter energy density parameter (Ω_m), curvature anisotropy parameter (Ω_σ), and dark energy parameter Ω_β as

$$\Omega_m = \frac{8\pi\rho}{3c^2H^2\phi}, \qquad \Omega_\sigma = \frac{k^2\phi^2}{3H^2A^6}, \qquad \Omega_\beta = \frac{\beta^2}{4H^2}. \tag{39}$$

The deceleration parameter (q) for scale factor and (q_ϕ) for scalar field are defined as [49]

$$q = -\frac{\ddot{a}}{aH^2}, \qquad q_\phi = -\frac{\ddot{\phi}}{\phi H^2}, \tag{40}$$

where $a(t) = A$ is the average scale factor.

Now, using Eq. (39) in (33), we get

$$\Omega_m + \Omega_\sigma + \Omega_\beta = 1 + \frac{\omega}{6}\xi^2 - \xi. \tag{41}$$

Again using Eqs. (39) and (40) in Eq. (34), we get

$$\gamma\Omega_m + \Omega_\sigma + \Omega_\beta = \frac{2}{3}q - \frac{1}{3} + \frac{\omega}{6}\xi^2 + \frac{2}{3}\xi - \frac{1}{3}q_\phi. \tag{42}$$

Equation (36) becomes

$$-q_\phi + 3\xi = \frac{3(1-3\gamma)\Omega_m}{2\omega+3}, \tag{43}$$

where $\xi = \frac{\dot{\phi}}{\phi H}$. From Eqs. (41)–(43), we get

$$q - \frac{(\omega - \omega\gamma - 3\gamma + 2)}{(1-3\gamma)}q_\phi + \frac{(3\omega - 3\omega\gamma - 12\gamma + 5)}{(1-3\gamma)}\xi = 2. \tag{44}$$

This gives the following power law relations between scalar field ϕ and scale factor A:

$$\phi = \phi_0\left(\frac{A}{A_0}\right)^{\frac{1-3\gamma}{\omega-\omega\gamma-3\gamma+2}} \tag{45}$$

and

$$\xi = \frac{1-3\gamma}{\omega - \omega\gamma - 3\gamma + 2}, \tag{46}$$

where A_0 and ϕ_0 are values of scale factor A and scalar field ϕ at present. Putting this value of ξ in Eq. (41), we get the following relationship for energy parameters:

$$\Omega_m + \Omega_\sigma + \Omega_\beta = 1 - \frac{(1-3\gamma)(5\omega - 3\omega\gamma - 18\gamma + 12)}{6(\omega - \omega\gamma - 3\gamma + 2)^2}. \tag{47}$$

In the Brans-Dicke theory as $\omega \to \infty$, we get the following relativistic result:

$$\Omega_m + \Omega_\sigma + \Omega_\beta = 1. \tag{48}$$

A. Gravitational constant versus redshift relation

As in the Brans-Dicke theory, gravitational constant G is reciprocal of ϕ, i.e.,

$$G = \frac{1}{\phi} \tag{49}$$

and

$$\frac{A_0}{A} = 1 + z, \tag{50}$$

where z is the redshift.

So, from Eqs. (45), (49), and (50), we obtain

$$\frac{G}{G_0} = (1+z)^{\frac{1-3\gamma}{\omega-\omega\gamma-3\gamma+2}}. \tag{51}$$

It is concluded that variation of the gravitational constant G over redshift z and coupling constant ω follows the same patterns for both isotropic and anisotropic BD universes.

This relationship shows that G grows toward the past, and in fact it diverges at cosmological singularity. Radar observations, lunar mean motion, and the Viking landers on Mars [52] suggest that the rate of variation of the gravitational constant must be very much slow of order 10^{-12} yr^{-1}. The recent experimental evidence [53,54] shows that $\omega > 3300$. Accordingly, we consider large coupling constant ω in this study.

From Eqs. (46) and (49), the present rate of the gravitational constant is calculated as

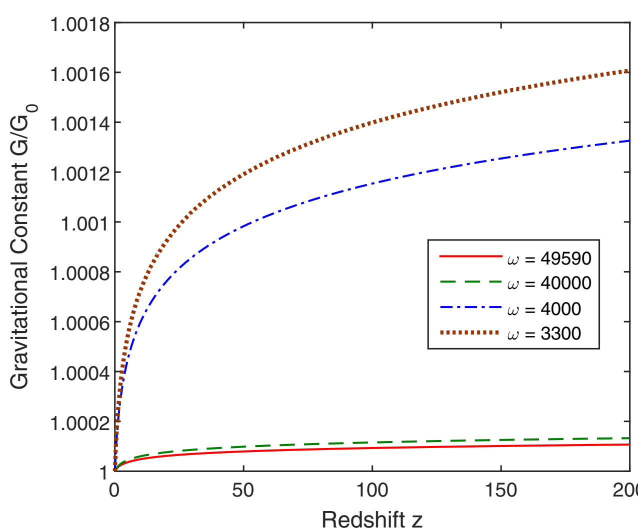

FIG. 1. Variation of gravitational constant over redshift.

$$\left(\frac{\dot{G}}{G}\right)_0 = -\frac{1-3\gamma}{\omega-\omega\gamma-3\gamma+2}H_0, \tag{52}$$

where $H_0 \approxeq 10^{-12}$ yr^{-1}.

Equation (51) exhibits the fact that G/G_0 varies over ω. For higher values of ω, G/G_0 grows very slow over redshift, whereas for lower values of ω it grows fast. The variations of the gravitational constant over the redshift for different ω's are shown in Fig. 1. From Fig. 1 and Eq. (51), it is clear that G/G_0 and in turn $\frac{1}{\phi}$ are increasing functions of redshift z for $0 \le \gamma \le \frac{1}{3}$. This implies that ϕ is a decreasing function of redshift z and so is an increasing function of cosmic time t. It means the value of G decreases with time due to background effects (i.e., scalar field). Also, as $\omega \to \infty$, $G/G_0 \to 1$, i.e., $G = G_0$ at $\omega = \infty$, and in this case the model behaves as an Einstein model in Lyra geometry.

IV. EXPRESSIONS FOR HUBBLE'S CONSTANT, LUMINOSITY DISTANCE, APPARENT MAGNITUDE, ETC

A. Hubble's Constant

The energy conservation Eq. (36) is integrable for constant EoS parameter ($\gamma = \text{const}$), giving rise to the following expression amongst matter density ρ, average scale factor $a(t) = A(t)$, and the redshift z of the universe:

$$\rho = \rho_0\left(\frac{A_0}{A}\right)^{3(1+\gamma)} = \rho_0(1+z)^{3(1+\gamma)}, \tag{53}$$

where we have used the relation given by Eq. (53).

Now, using Eqs. (38), (47), (50), and (53), we get following expressions for Hubble's constant in terms of scale factor and redshift:

$$H = \frac{H_0}{\sqrt{1-\frac{(1-3\gamma)(5\omega-3\omega\gamma-18\gamma+12)}{6(\omega-\omega\gamma-3\gamma+2)^2}}}\sqrt{\Omega_{m0}\left(\frac{A_0}{A}\right)^{\frac{3\omega-3\omega\gamma^2+6\gamma+7}{\omega-\omega\gamma-3\gamma+2}} + \Omega_{\sigma0}\left(\frac{A_0}{A}\right)^{\frac{2(3\omega-3\omega\gamma-6\gamma+5}{\omega-\omega\gamma-3\gamma+2}} + \Omega_{\beta0}} \tag{54}$$

and

$$H = \frac{H_0}{\sqrt{1-\frac{(1-3\gamma)(5\omega-3\omega\gamma-18\gamma+12)}{6(\omega-\omega\gamma-3\gamma+2)^2}}}\sqrt{\Omega_{m0}(1+z)^{\frac{3\omega-3\omega\gamma^2+6\gamma+7}{\omega-\omega\gamma-3\gamma+2}} + \Omega_{\sigma0}(1+z)^{\frac{2(3\omega-3\omega\gamma-6\gamma+5}{\omega-\omega\gamma-3\gamma+2}} + \Omega_{\beta0}}, \tag{55}$$

respectively. The graph of Hubble constant against redshift is shown in Fig. 2.

B. Luminosity distance

The luminosity distance which determines the flux of the source is given by

$$D_L = A_0 r(1+z), \tag{56}$$

where r is the spatial coordinate distance of a source. The luminosity distance for metric (16) can be written as [49]

$$D_L = c(1+z)\int_0^z \frac{dz}{H(z)}. \tag{57}$$

Therefore, by using Eq. (55), the luminosity distance D_L for our model is obtained as

$$D_L = \frac{c(1+z)\sqrt{1-\frac{(1-3\gamma)(5\omega-3\omega\gamma-18\gamma+12)}{6(\omega-\omega\gamma-3\gamma+2)^2}}}{H_0}\int_0^z \frac{dz}{\sqrt{\Omega_{m0}(1+z)^{\frac{3\omega-3\omega\gamma^2+6\gamma+7}{\omega-\omega\gamma-3\gamma+2}} + \Omega_{\sigma0}(1+z)^{\frac{2(3\omega-3\omega\gamma-6\gamma+5}{\omega-\omega\gamma-3\gamma+2}} + \Omega_{\beta0}}}. \tag{58}$$

C. Apparent magnitude

The apparent magnitude of a source of light is related to the luminosity distance via the following expression:

$$m = 16.08 + 5\log_{10}\frac{H_0 D_L}{0.026cMpc}. \tag{59}$$

TABLE I. Outcomes of the R^2 test for the best fit curve of apparent magnitude $m(z)$ in Eq. (60) and Hubble constant $H(z)$ in Eq. (55) and Figs. 4 and 2. The values of coefficients Ω_m, Ω_σ, Ω_β, and ω are at 95% confidence of bounds.

Function	γ	ω	Ω_{m0}	$\Omega_{\sigma 0}$	$\Omega_{\beta 0}$	H_0	R^2	RMSE
$H(z)$	$0 \leq \gamma \leq \frac{1}{3}$	49590	0.2991	2.341×10^{-14}	0.7443	71.27	0.8798	16.75
$m(z)$	$0 \leq \gamma \leq \frac{1}{3}$	49413	0.2940	1.701×10^{-14}	0.7452	$\cdots$	0.9931	0.2664

Using Eq. (58), we get the following expression for the apparent magnitude in our model

$$m = 16.08 + 5\log_{10}\left((1+z)\sqrt{1-\frac{(1-3\gamma)(5\omega-3\omega\gamma-18\gamma+12)}{6(\omega-\omega\gamma-3\gamma+2)^2}}\int_0^z \frac{dz}{\sqrt{\Omega_{m0}(1+z)^{\frac{3\omega-3\omega\gamma^2+6\gamma+7}{\omega-\omega\gamma-3\gamma+2}}+\Omega_{\sigma 0}(1+z)^{\frac{2(3\omega-3\omega\gamma-6\gamma+5}{\omega-\omega\gamma-3\gamma+2}}+\Omega_{\beta 0}}}\right). \tag{60}$$

D. Energy parameters at present

We consider 580 high redshift ($0.015 \leq z \leq 1.414$) SN Ia supernova data of observed apparent magnitudes along with their possible errors from the union 2.1 compilation [55]. In our present study, we have used a technique to estimate the present values of energy parameters Ω_{m0}, $\Omega_{\sigma 0}$, and $\Omega_{\beta 0}$ by comparing the theoretical and observed results with the help of the R^2 formula,

$$R^2_{\mathrm{SN}} = 1 - \frac{\sum_{i=1}^{580}[(m_i)_{\mathrm{ob}} - (m_i)_{\mathrm{th}}]^2}{\sum_{i=1}^{580}[(m_i)_{\mathrm{ob}} - (m_i)_{\mathrm{mean}}]^2}. \tag{61}$$

Here the sums are taken over datasets of observed and theoretical values of the apparent magnitude of 580 supernovae.

The ideal case $R^2 = 1$ occurs when the observed data and theoretical function $m(z)$ agree exactly. On the basis of the maximum value of R^2, we get the best fit present values of Ω_m, Ω_σ, and Ω_β for the apparent magnitude $m(z)$ function as shown in Eq. (60) which is given in Table I. For this, coupling constant ω is taken as > 40000 and the theoretical values are calculated from Eq. (60). We have found the best fit present values of Ω_m, Ω_σ, and Ω_β are $(\Omega_m)_0 = 0.2940$, $(\Omega_\sigma)_0 = 1.701 \times 10^{-14}$, and $(\Omega_\beta)_0 = 0.7452$ for maximum $R^2 = 0.9931$ with root mean square error (RMSE) 0.2664, i.e., $m(z) \pm 0.2664$, and their R^2 values only 0.69% far from the best one. Figures 3 and 4 indicate how the observed values of luminosity distances and apparent magnitudes, respectively, reach close to the theoretical graphs for $(\Omega_m)_0 = 0.2940$, $(\Omega_\sigma)_0 = 1.701 \times 10^{-14}$, $(\Omega_\beta)_0 = 0.7452$.

E. Estimation of present values of Hubble's constant H_0

We present a dataset of the observed values of the Hubble parameter $H(z)$ versus the redshift z with possible errors in the form of Table II. These data points were obtained by various researchers from time to time, by using the different ages approach.

In our model, Hubble's constant $H(z)$ versus redshift z relation Eq. (55) is reduced to

$$H^2 = (1.0003)H_0^2[0.2991(1+z)^3 + 2.341 \times 10^{-14}(1+z)^6 + 0.7443], \tag{62}$$

where we have taken $(\Omega_m)_0 = 0.2991$, $(\Omega_\sigma)_0 = 2.341 \times 10^{-14}$, $(\Omega_\beta)_0 = 0.7443$, and the coupling constant $\omega = 49590$. The Hubble Space Telescope (HST) observations of Cepheid variables [60] provide present values of Hubble constant H_0 in the range $H_0 = 73.8 \pm 2.4$ km/s/Mpc. A large number

TABLE II. Hubble's constant table.

z	$H(z)$	σ_H	Reference	Method
0.07	69	19.6	Moresco *et al.* [56]	DA
0.1	69	12	Zhang *et al.* [57]	DA
0.12	68.6	26.2	Moresco *et al.* [56]	DA
0.17	83	8	Zhang *et al.* [57]	DA
0.28	88.8	36.6	Moresco *et al.* [56]	DA
0.4	95	17	Zhang *et al.* [57]	DA
0.48	97	62	Zhang *et al.* [57]	DA
0.593	104	13	Moresco [58]	DA
0.781	105	12	Moresco [58]	DA
0.875	125	17	Moresco [58]	DA
0.88	90	40	Zhang *et al.* [57]	DA
0.9	117	23	Zhang *et al.* [57]	DA
1.037	154	20	Moresco [58]	DA
1.3	168	17	Zhang *et al.* [57]	DA
1.363	160	33.6	Moresco [58]	DA
1.43	177	18	Zhang *et al.* [57]	DA
1.53	140	14	Zhang *et al.* [57]	DA
1.75	202	40	Zhang *et al.* [57]	DA
1.965	186.5	50.4	Stern *et al.* [59]	DA

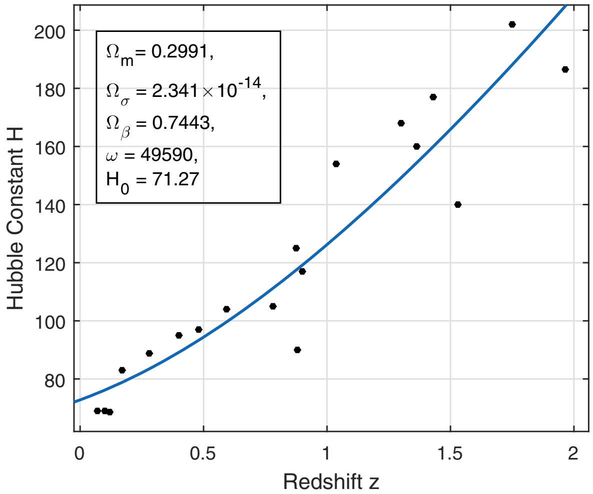

FIG. 2. Hubble constant versus redshift best fit curve.

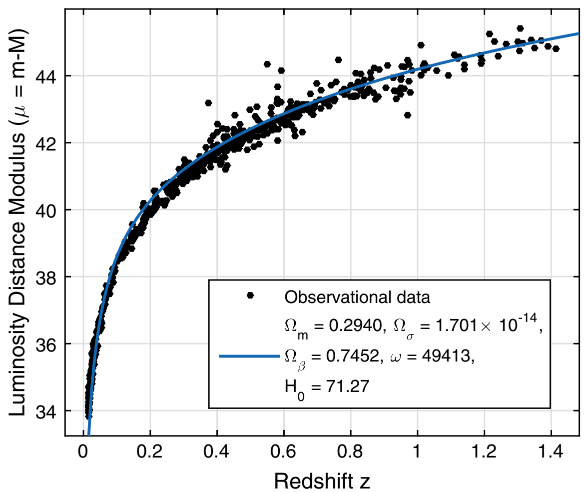

FIG. 3. Luminosity distance modulus versus redshift best fit curve.

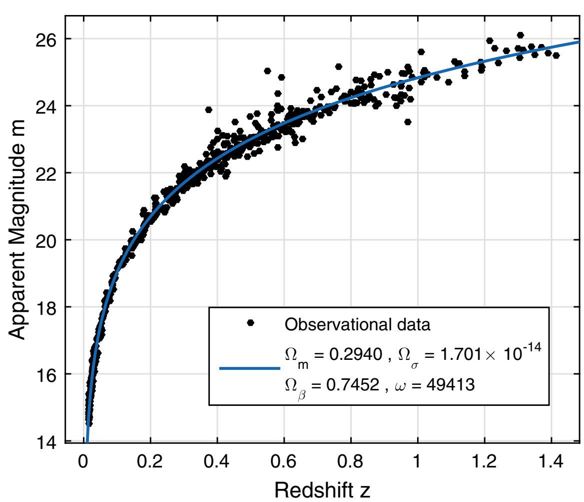

FIG. 4. Apparent magnitude versus redshift best fit curve.

of datasets of theoretical values of Hubble constant $H(z)$ versus z, corresponding to H_0 in the range $(60.45 \leq H_0 \leq 74.21)$ are obtained by using Eq. (62). It should be noted that the redshift z's are taken from Table II and each dataset consists of 19 data points. In order to get the best fit theoretical dataset of Hubble's constant $H(z)$ versus z, we calculate the R^2 test by using the following statistical formula:

$$R^2_{\mathrm{SN}} = 1 - \frac{\sum_{i=1}^{19}[(H_i)_{\mathrm{ob}} - (H_i)_{\mathrm{th}}]^2}{\sum_{i=1}^{19}[(H_i)_{\mathrm{ob}} - (H_i)_{\mathrm{mean}}]^2}. \tag{63}$$

Here the sums are taken over datasets of observed and theoretical values of Hubble's constants. The observed values are taken from Table II and theoretical values are calculated from Eq. (55). Using the above R^2 test, we have found the best fit function of $H(z)$ for Eq. (55) which is mentioned in Table I.

From Table I, one can see that the best fit value of Hubble constant H_0 is 71.27 for maximum $R^2 = 0.8798$ with root mean square error RMSE $= 16.75$, i.e., $H_0 = 71.27 \pm 16.75$ and their R^2 values only 12.02% far from the best one. Figure 2 shows the dependence of Hubble's constant with redshift. Hubble's observed data points are closed to the graph corresponding to $(\Omega_m)_0 = 0.2991$, $(\Omega_\sigma)_0 = 2.341 \times 10^{-14}$, and $(\Omega_\beta)_0 = 0.7443$. This validates the proximity of observed and theoretical values.

V. ESTIMATION OF CERTAIN OTHER PHYSICAL PARAMETERS OF THE UNIVERSE

A. Matter, dark energy, and anisotropic energy densities

The matter, anisotropic energy, and dark energy densities of the universe are related to the energy parameters through the following equation:

$$\Omega_m = \frac{\rho_m}{\rho_c}, \qquad \Omega_\sigma = \frac{\rho_\sigma}{\rho_c}, \qquad \Omega_\beta = \frac{\rho_\beta}{\rho_c}, \tag{64}$$

where

$$\rho_c = \frac{3c^2H^2}{8\pi G} = \frac{3c^2\phi H^2}{8\pi}. \tag{65}$$

So,

$$(\rho_m)_0 = (\rho_c)_0(\Omega_m)_0, \qquad (\rho_\sigma)_0 = (\rho_c)_0(\Omega_\sigma)_0,$$
$$(\rho_\beta)_0 = (\rho_c)_0(\Omega_\beta)_0. \tag{66}$$

Now the present value of ρ_c is obtained as

$$(\rho_c)_0 = \frac{3c^2H_0^2}{8\pi G} = 1.88h_0^2 \times 10^{-29}\ \mathrm{gm/cm^3}. \tag{67}$$

The estimated value of $h_0 = 0.7127$. Therefore, the present value of matter and dark energy densities are given by

$$(\rho_m)_0 = 0.562308 h_0^2 \times 10^{-29}\ \mathrm{gm/cm^3}, \tag{68}$$

$$(\rho_\sigma)_0 = 4.40108 h_0^2 \times 10^{-43}\ \mathrm{gm/cm^3}, \tag{69}$$

$$(\rho_\beta)_0 = 1.399284 h_0^2 \times 10^{-29}\ \mathrm{gm/cm^3}. \tag{70}$$

Here, we have taken $(\Omega_m)_0 = 0.2991$, $(\Omega_\sigma)_0 = 2.341 \times 10^{-14}$, and $(\Omega_\beta)_0 = 0.7443$. General expressions for energy densities are given by

$$\rho = \rho_0 \left(\frac{a_0}{a}\right)^{3(1+\gamma)} = \rho_0 (1+z)^{3(1+\gamma)}, \tag{71}$$

$$\rho_\sigma = \frac{k^2 c^2 \phi^3}{8\pi} \left(\frac{a_0}{a}\right)^6 = \frac{k^2 c^2 \phi^3}{8\pi} (1+z)^6, \tag{72}$$

and

$$\rho_\beta = (\rho_c)\Omega_\beta = \frac{3c^2\beta^2}{32\pi}\phi. \tag{73}$$

From above, we observe that the current matter and dark energy densities are very close to the values predicted by the various surveys described in the Introduction.

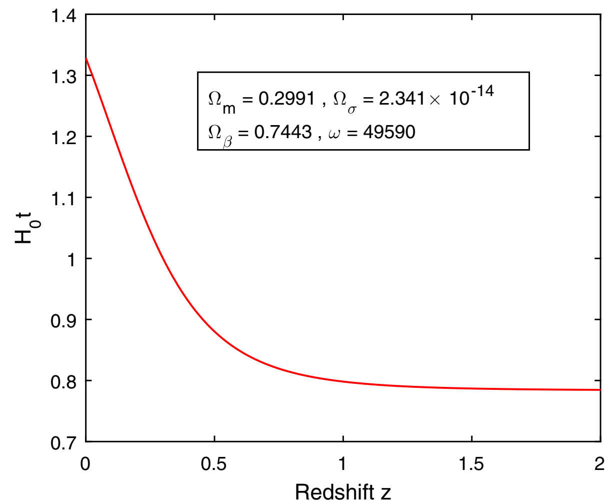

FIG. 5. Plot of $H_0 t$ versus redshift z.

B. Age of the universe

By using the standard formula

$$t = \int_0^t dt = \int_0^A \frac{dA}{AH},$$

we obtain the values of t in terms of the scale factor and redshift, respectively,

$$t = \int_0^A \frac{\sqrt{1 - \frac{(1-3\gamma)(5\omega-3\omega\gamma-18\gamma+12)}{6(\omega-\omega\gamma-3\gamma+2)^2}}\,dA}{AH_0\sqrt{\Omega_{m0}(\frac{A_0}{A})^{\frac{3\omega-3\omega\gamma^2+6\gamma+7}{\omega-\omega\gamma-3\gamma+2}} + \Omega_{\sigma0}(\frac{A_0}{A})^{\frac{2(3\omega-3\omega\gamma-6\gamma+5}{\omega-\omega\gamma-3\gamma+2}} + \Omega_{\beta0}}}, \tag{74}$$

$$t = \int_0^z \frac{\sqrt{1 - \frac{(1-3\gamma)(5\omega-3\omega\gamma-18\gamma+12)}{6(\omega-\omega\gamma-3\gamma+2)^2}}\,dz}{(1+z)H_0\sqrt{\Omega_{m0}(1+z)^{\frac{3\omega-3\omega\gamma^2+6\gamma+7}{\omega-\omega\gamma-3\gamma+2}} + \Omega_{\sigma0}(1+z)^{\frac{2(3\omega-3\omega\gamma-6\gamma+5}{\omega-\omega\gamma-3\gamma+2}} + \Omega_{\beta0}}}. \tag{75}$$

For $\omega = 49590$, $(\Omega_m)_0 = 0.2991$, $(\Omega_\sigma)_0 = 2.341 \times 10^{-14}$, and $(\Omega_\beta)_0 = 0.7443$, Eq. (75) gives $t_0 \to 1.3282 H_0^{-1}$ for high redshift. This means that the present age of the universe is $t_0 = 18.23^{+5.60}_{-3.47}$ Gyrs as per our model. From WMAP data, the empirical value of the present age of the universe is 13.73 ± 0.13 Gyrs which is closed to the present age of the universe, estimated by us in this paper.

Figure 5 shows the variation of time over redshift. At $z = 0$ the value of $H_0 t_0 = 1.3282$. This provides the present age of the universe. This also indicated the consistency with recent observations.

C. Deceleration parameter

From Eqs. (41), (44), and (46), we obtain the expressions for DP as

$$q = -\frac{\omega + \omega\gamma + 1}{2\omega\gamma + 3\gamma - 2\omega - 3} + \frac{(\omega - 3\omega\gamma + 2)(1 - 3\gamma)}{2(\omega - \omega\gamma - 3\gamma + 2)(2\omega\gamma + 3\gamma - 2\omega - 3)} + \frac{3(\omega - \omega\gamma - 3\gamma + 2)}{2\omega\gamma + 3\gamma - 2\omega - 3}(\gamma\Omega_m + \Omega_\sigma + \Omega_\beta). \tag{76}$$

Using Eqs. (38), (46), (54), and (55) in Eq. (76), we get the following expression for the deceleration parameter:

$$q = -\frac{\omega + \omega\gamma + 1}{2\omega\gamma + 3\gamma - 2\omega - 3} + \frac{(\omega - 3\omega\gamma + 2)(1 - 3\gamma)}{2(\omega - \omega\gamma - 3\gamma + 2)(2\omega\gamma + 3\gamma - 2\omega - 3)} + \frac{3(\omega - \omega\gamma - 3\gamma + 2)}{2\omega\gamma + 3\gamma - 2\omega - 3} \frac{\left(1 - \frac{(1-3\gamma)(5\omega - 3\omega\gamma - 18\gamma + 12)}{6(\omega - \omega\gamma - 3\gamma + 2)^2}\right)\left[\gamma\Omega_{m0}\left(\frac{A_0}{A}\right)^{\frac{3\omega - 3\omega\gamma^2 + 6\gamma + 7}{\omega - \omega\gamma - 3\gamma + 2}} + \Omega_{\sigma 0}\left(\frac{A_0}{A}\right)^{\frac{2(3\omega - 3\omega\gamma - 6\gamma + 5)}{\omega - \omega\gamma - 3\gamma + 2}} + \Omega_{\beta 0}\right]}{\left[\Omega_{m0}\left(\frac{A_0}{A}\right)^{\frac{3\omega - 3\omega\gamma^2 + 6\gamma + 7}{\omega - \omega\gamma - 3\gamma + 2}} + \Omega_{\sigma 0}\left(\frac{A_0}{A}\right)^{\frac{2(3\omega - 3\omega\gamma - 6\gamma + 5)}{\omega - \omega\gamma - 3\gamma + 2}} + \Omega_{\beta 0}\right]}. \tag{77}$$

In terms of redshift, q is given by

$$q = -\frac{\omega + \omega\gamma + 1}{2\omega\gamma + 3\gamma - 2\omega - 3} + \frac{(\omega - 3\omega\gamma + 2)(1 - 3\gamma)}{2(\omega - \omega\gamma - 3\gamma + 2)(2\omega\gamma + 3\gamma - 2\omega - 3)} + \frac{3(\omega - \omega\gamma - 3\gamma + 2)}{2\omega\gamma + 3\gamma - 2\omega - 3} \frac{\left(1 - \frac{(1-3\gamma)(5\omega - 3\omega\gamma - 18\gamma + 12)}{6(\omega - \omega\gamma - 3\gamma + 2)^2}\right)\left[\gamma\Omega_{m0}(1+z)^{\frac{3\omega - 3\omega\gamma^2 + 6\gamma + 7}{\omega - \omega\gamma - 3\gamma + 2}} + \Omega_{\sigma 0}(1+z)^{\frac{2(3\omega - 3\omega\gamma - 6\gamma + 5)}{\omega - \omega\gamma - 3\gamma + 2}} + \Omega_{\beta 0}\right]}{\left[\Omega_{m0}(1+z)^{\frac{3\omega - 3\omega\gamma^2 + 6\gamma + 7}{\omega - \omega\gamma - 3\gamma + 2}} + \Omega_{\sigma 0}(1+z)^{\frac{2(3\omega - 3\omega\gamma - 6\gamma + 5)}{\omega - \omega\gamma - 3\gamma + 2}} + \Omega_{\beta 0}\right]}. \tag{78}$$

As the present phase ($z = 0$) of the universe is accelerating $q \leq 0$, i.e., $\frac{\ddot{a}}{a} \geq 0$, so we must have

$$\Omega_{\beta 0} \geq \left[\frac{-3\gamma^2 + 4\gamma + 1}{2(\gamma + 2)} + \frac{3(\gamma - 1)[-24\gamma^2 + 8\gamma + 4 - \omega(9\gamma^3 - 21\gamma^2 + 7\gamma - 3)]}{2(\gamma + 2)[(12\gamma^2 - 36\gamma + 24)\omega^2 + (45\gamma^2 - 126\gamma + 73)\omega - 60\gamma + 44]}\right]\Omega_{m0} - \Omega_{\sigma 0}. \tag{79}$$

For $\omega = 49590$ and $\Omega_m = 0.2991$, $\Omega_\sigma = 2.341 \times 10^{-14}$, $0 \leq \gamma < \frac{1}{3}$ the minimum value of $\Omega_{\beta 0}$ is given by $\Omega_{\beta 0} \geq 0.3152$ which is consistent with the present observed value of $\Omega_{\beta 0} = 0.7443$. Putting $z = 0$ in Eq. (79), the present value of the deceleration parameter is obtained as

$$q_0 = -0.57. \tag{80}$$

Equation (79) also provides

$$z_c \approx 0.708 \quad \text{at } q = 0. \tag{81}$$

Therefore, the universe attains the accelerating phase when $z < z_c$.

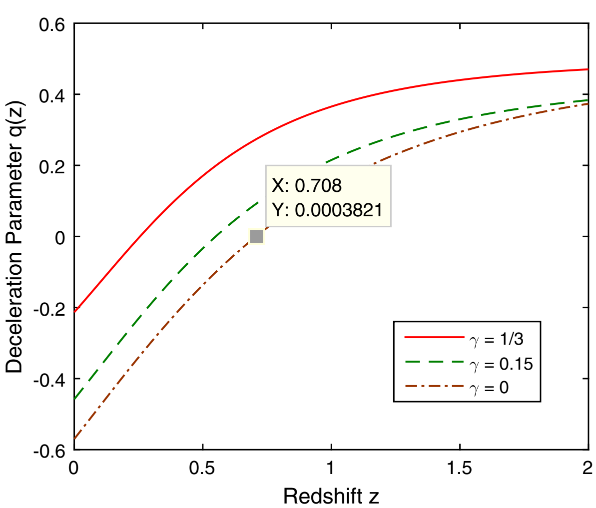

FIG. 6. Variation of deceleration parameter versus redshift.

Converting redshift into time from Eq. (81), the value of z_c is reduced to

$$z_c = 0.708 \sim 0.8258 H_0^{-1} \text{ Gyrs} \sim 11.33 \text{ Gyrs} \tag{82}$$

So, the acceleration must have begun in the past at 11.33 Gyrs. Figure 6 shows how the deceleration parameter increases from negative to positive over redshift which means that in the past the universe was decelerating, and at a instant $z_c \cong 708$, it became stationary; thereafter it goes on accelerating.

D. Shear scalar

The shear scalar is given by

$$\sigma^2 = \frac{1}{2}\sigma_{ij}\sigma^{ij}, \tag{83}$$

where

$$\sigma_{ij} = u_{i;j} - \theta(g_{ij} - u_i u_j). \tag{84}$$

In our model

$$\sigma^2 = \frac{\dot{d}^2}{d^2} = \frac{k^2\phi^2}{A^6} = (\Omega_\sigma)_0 H_0^2 (1+z)^{\frac{2(3\omega - 3\omega\gamma - 6\gamma + 5)}{\omega - \omega\gamma - 3\gamma + 2}}. \tag{85}$$

From Eq. (85), it is clear that the shear scalar vanishes as $A \to \infty$.

E. Relative anisotropy

The relative anisotropy is given by

$$\frac{\sigma^2}{\rho_m} = \frac{3\Omega_{\sigma 0} H_0^2 (1+z)^{\frac{2(3\omega-3\omega\gamma-6\gamma+5)}{\omega-\omega\gamma-3\gamma+2}}}{(\rho_c)_0 \Omega_{m0}}. \tag{86}$$

This follows the same pattern as the shear scalar. This means that relative anisotropy decreases over the scale factor, i.e., time.

VI. DISCUSSION OF RESULTS

For the viability of a cosmological model, it is necessary that it should be consistent with recent observational data. From the analysis of various observational data, some of the basic observational parameters Ω_0, q_0, and H_0 read as the total density parameter, deceleration parameter, and Hubble constant, respectively, are evaluated. On the basis of these, it has been established now that the expansion of the universe is in an accelerating phase at present. Since there is not enough matter or radiation to lead this accelerated expansion, theoreticians attributed this to a mysterious form of energy present in the universe and termed it as dark energy (DE). The earlier discarded cosmological constant Λ is reintroduced to incorporate DE. But the question is, what is the actual nature of this dark energy and from where does the Λ-term come? To answer this, various researchers using different approaches, proposed different models, but despite these, it is still a mystery for the researchers.

In this order, in the present paper, we have proposed a cosmological model of the universe in Bianchi type-I spacetime in the context of an amalgamation of BD theory and Lyra geometry. The Lyra geometry establishes a term such as cosmological constant Λ, which otherwise is simply added in the Einstein field equation by Einstein and in some other theories. The BD theory is involved by making the model consistent with Mach's principle, since Einstein's GR and also Lyra's modification are inconsistent with it. Here, we have solved the field equations (17) to (21) by aking EoS parameter $\gamma = \text{const}$. We have defined the energy density parameters: Ω_m as the matter energy density parameter, Ω_σ as the curvature energy density parameter, and Ω_β as the dark energy density parameter. Since the observational data are available in the form of the apparent magnitude and Hubble constant H with redshift z, therefore, we have derived the expressions for the apparent magnitude $m(z)$ and Hubble constant $H(z)$ in terms of energy parameters Ω_m, Ω_σ, Ω_β and redshift z as in Eqs. (60) and (55), respectively.

For mapping the theoretical model to the observed universe model we have fitted the curve of the Hubble constant $H(z)$ and apparent magnitude $m(z)$ using the R^2-test formula. On the basis of the maximum R^2 value, we obtained the best fit curve for $m(z)$ to 580 data of the union 2.1 compilation data of SNe Ia observations [55], with coefficients $\Omega_m = 0.2940$, $\Omega_\sigma = 1.701 \times 10^{-14}$, $\Omega_\beta = 0.7452$, and $\omega = 49413$ with 95% confidence of bounds and maximum $R^2 = 0.9931$. On the other hand, we have found the best fit curve for $H(z)$ with coefficients $\Omega_m = 0.2991$, $\Omega_\sigma = 2.341 \times 10^{-14}$, $\Omega_\beta = 0.7443$, $H_0 = 71.27$, and $\omega = 49590$ with the maximum $R^2 = 0.8798$. From these two fittings (mentioned in Table I) with different sources of datasets, one can see that the values of density parameters Ω_m, Ω_σ, Ω_β are approximately compatible with each other. If we compare these values with the values obtained from the analysis of the observational datasets, we find that these are very close to them. From Eq. (47), one can see that the total energy density parameter is greater than unity, which means our model supports an open universe.

In Sec. V. 3, we have obtained the expression for the deceleration parameter $q(z)$ in Eq. (78) in terms of density parameters and redshift z. Figure 6 represents the plot of DP versus redshift z with coefficients $\Omega_m = 0.2991$, $\Omega_\sigma = 2.341 \times 10^{-14}$, $\Omega_\beta = 0.7443$, and $\omega = 49590$ for $\gamma = 0.3$, 0.15, 0. From Fig. 6, one can see that $q(z)$ is an increasing function of redshift z. A nonzero deceleration parameter $q(z)$ depicts the expansion phase of the universe (decelerating or accelerating, as its value is positive or negative, respectively). Here, from Fig. 6, one can see that the signature of q changes at $z_c \approx 0.7080$, and this point is called the transition point of the model. For $z > z_c = 0.708$, $q > 0$ indicates the universe is in the decelerating phase, and for $z < z_c = 0.708$, $q < 0$ indicates the expansion is in the accelerating phase. It means the expansion of the universe is entered into the accelerating phase at $z \approx 0.708$ [see Eq. (81)] which is equivalent to the age of 11.33 Gyrs [see Eq. (82)]. The direct empirical evidence for the transition from past deceleration to present acceleration is provided by SNe type Ia measurements. In their preliminary analysis it was found that the SNe data favor recent acceleration ($z < 0.5$) and past deceleration ($z > 0.5$). More recently, the High-z Supernova Search (HZSNS) team has obtained $z_t = 0.46 \pm 0.13$ at (1σ) confidence level [61] in 2004 which has been further improved to $z_t = 0.43 \pm 0.07$ at (1σ) confidence level [61] in 2007. The Supernova Legacy Survey (SNLS) (Astier *et al.* [62]), as well as the one recently compiled by Davis *et al.* [63] (in better agreement with the flat ΛCDM model $z_t = (2\Omega_\Lambda/\Omega_m)^{\frac{1}{3}} - 1 \sim 0.66$), yields a transition redshift $z_t \sim 0.6(1\sigma)$. Another limit is $0.60 \leq z_t \leq 1.18$ (2σ, joint analysis) [64]. Also, in Eq. (80), we see that at $z = 0$ (denoting the present stage of the universe) $q = -0.57$, which is in good agreement with recent observations.

In Sec. V. 2, we have estimated the present age of the universe, which comes out to be $t_0 \to 1.3282 H_0^{-1}$, for $\omega = 49590$, $(\Omega_m)_0 = 0.2991$, $(\Omega_\sigma)_0 = 2.341 \times 10^{-14}$, and $(\Omega_\beta)_0 = 0.7443$, which is closed to the empirical value from WMAP data.

So, we can say that these estimations establish the viability of our model.

VII. CONCLUSION

We summarize our results by presenting Table III which displays the values of cosmological parameters at present obtained by us. We have found the following main features of the model:

(i) The derived model is an anisotropic Bianchi type-I universe which tends to the isotropic flat ΛCDM model at the late time because of $\Omega_{\sigma 0} \approx 0$ and shear scalar $\sigma^2 \to 0$ as $A \to \infty$.

(ii) The values of density parameters Ω_{m0}, $\Omega_{\sigma 0}$, and $\Omega_{\beta 0}$ obtained are very close to $H(z)$ and SNe Ia data. It declares the viability of the model.

(iii) The present values of various physical parameters calculated and presented in Table III are in good agreement with the recent observations.

(iv) The deceleration parameter shows signature flipping (from positive to negative with decreasing redshift; see Fig. 6), i.e., the transition phase at $z_c \approx 0.7080$ which is in good agreement with various relativistic models and cosmological surveys.

(v) We have found that the acceleration would have begun in the past at $11.33^{+3.48}_{-3.16}$ Gyrs.

(vi) The Lyra geometry with a constant displacement vector removes the cosmological constant Λ-term problem naturally.

(vii) The present universe is dominated by scalar field ϕ, and it is the responsible candidate for the present behavior of the universe.

TABLE III. Cosmological parameters at present for $0 \leq \gamma < \frac{1}{3}$.

Cosmological parameters	Values at present
BD coupling constant ω	49590
Matter energy parameter Ω_{m0}	0.2991
Dark energy parameter $\Omega_{\beta 0}$	0.7443
Anisotropic energy parameter $\Omega_{\sigma 0}$	2.341×10^{-14}
Hubble's constant H_0	71.27
Deceleration parameter q_0	−0.57
Matter energy density ρ_{m0}	$0.562308h_0^2 \times 10^{-29}$ gm/cm^3
Dark energy density $\rho_{\beta 0}$	$1.39928h_0^2 \times 10^{-29}$ gm/cm^3
Anisotropic energy density $\rho_{\sigma 0}$	$4.40108h_0^2 \times 10^{-43}$ gm/cm^3
Age of the universe t_0	$18.23^{+5.60}_{-3.47}$ Gyrs

These results are in good agreement with the various observational results described in the Introduction. In the present model, the energy parameter Ω_β behaves like the dark energy parameter Ω_Λ. The model creates more interest in researchers to study the behavior of gauge function β and scalar field ϕ and their coupling in formulation of the universe model.

ACKNOWLEDGMENTS

The authors are thankful to IASE (Deemed to be University), Sardarshahar, Rajsthan, and GLA University, Mathura, Uttar Pradesh, India, for providing facilities and support where part of this work is carried out.

[1] H. Weyl, Sitzungsber. Preuss. Akad. Wiss. Berlin (Math.-Phys.) **1918**, 465 (1918).
[2] G. Lyra, Math. Z. **54**, 52 (1951).
[3] E. Scheibe, Math. Z. **57**, 65 (1952).
[4] D. K. Sen, Z. Phys. **149**, 311 (1957).
[5] D. K. Sen and K. A. Dunn, J. Math. Phys. (N.Y.) **12**, 578 (1971).
[6] C. Brans and R. H. Dicke, Phys. Rev. **124**, 925 (1961).
[7] R. H. Dicke, Phys. Rev. **125**, 2163 (1962).
[8] W. D. Halford, Aust. J. Phys. **23**, 863 (1970).
[9] W. D. Halford, J. Math. Phys. (N.Y.) **13**, 1699 (1972).
[10] G. F. R. Ellis and R. Maartens, Classical Quantum Gravity **21**, 223 (2004).
[11] G. F. R. Ellis, J. Murugan, and C. G. Tsagas, Classical Quantum Gravity **21**, 233 (2004).
[12] S. Mukherjee, B. C. Paul, N. K. Dadhich, S. D. Maharaj, and A. Beesham, Classical Quantum Gravity **23**, 6927 (2006).
[13] D. K. Sen, Z. Phys. **149**, 311 (1957).
[14] D. K. Sen and K. A. Dunn, J. Math. Phys. (N.Y.) **12**, 578 (1971).
[15] K. S. Bhamra, Aust. J. Phys. **27**, 541 (1974).
[16] S. B. Kalyanshetti and B. B. Waghmode, Gen. Relativ. Gravit. **14**, 823 (1982).
[17] D. R. K. Reddy and P. Innaiah, Astrophys. Space Sci. **114**, 285 (1985).
[18] D. R. K. Reddy and R. Venkateswarlu, Astrophys. Space Sci. **136**, 183 (1987).
[19] A. Beesham, Astrophys. Space Sci. **127**, 355 (1986).
[20] A. Beesham, Aust. J. Phys. **41**, 833 (1988).
[21] A. Pradhan and S. S. Kumhar, Astrophys Space Sci. **321**, 137 (2009).
[22] A. Pradhan and P. Mathur, Fizika B **18**, 243 (2009).
[23] A. Pradhan and P. Yadav, Int. J. Math. Math. Sci. **2009**, 471938 (2009).
[24] A. Pradhan, J. Math. Phys. (N.Y.) **50**, 022501 (2009).
[25] A. Pradhan, H. Amirhashehi, and H. Zanuddin, Int. J. Theor. Phys. **50**, 56 (2011).
[26] A. Pradhan and A. K. Singh, Int. J. Theor. Phys. **50**, 916 (2011).
[27] A. K. Yadav, Fizika B **19**, 53 (2010).
[28] S. Agarwal, R. K. Pandey, and A. Pradhan, Int. J. Theor. Phys. **50**, 296 (2011).

[29] R. S. Singh and A. Singh, Electron. J. Theor. Phys. **9**, 265 (2012).
[30] A. G. Riess *et al.*, Astron. J. **116**, 1009 (1999).
[31] S. Perlmutter *et al.*, Astrophys. J. **517**, 565 (1999).
[32] D. Spergel *et al.*, Astrophys. J. Suppl. Ser. **148**, 175 (2003).
[33] E. Komatsu *et al.*, Astrophys. J. Suppl. Ser. **192**, 18 (2011).
[34] C. Blake and K. Glazebrook, Astrophys. J. **594**, 665 (2003).
[35] H. Seo and D. Eisenstein, Astrophys. J. **598**, 720 (2003).
[36] G. R. Dvali, G. Gabadadze, and M. Porrati, Phys. Lett. B **485**, 208 (2000).
[37] S. Nojiri and S. D. Odintsov, Phys. Rev. D **68**, 123512 (2003).
[38] S. Capozziello, Int. J. Mod. Phys. D **11**, 483 (2002).
[39] P. S. Apostolopoulos, N. Brouzakis, E. N. Saridakis, and N. Tetradis, Phys. Rev. D **72**, 044013 (2005).
[40] S. Nojiri and S. D. Odintsov, Int. J. Geom. Methods Mod. Phys. **04**, 115 (2007).
[41] F. K. Diakonos and E. N. Saridakis, J. Cosmol. Astropart. Phys. 02 (2009) 030.
[42] Abdussatter and S. R. Prajapati, Astrophys. Space Sci. **331**, 657 (2011).
[43] C. L. Bennet *et al.*, Astrophys. J. Suppl. Ser. **148**, 1 (2003).
[44] A. G. Riess *et al.*, Astrophys. J. **607**, 665 (2004).
[45] P. Astier *et al.*, Astron. Astrophys. **447**, 31 (2006).
[46] D. Rapetti, S. W. Allen, M. Amin, and R. D. Blandford, Mon. Not. R. Astron. Soc. **375**, 1510 (2007).
[47] R. Garcia-Salcedo, T. Gonzalez, and I. Quiros, Phys. Rev. D **89**, 084047 (2014).
[48] V. Sahni, T. D. Saini, A. A. Starobinsky, and U. Alam, JETP Lett. **77**, 201 (2003).
[49] G. K. Goswami, M. Mishra, and A. K. Yadav, Int. J. Theor. Phys. **54**, 315 (2015).
[50] R. Zia and D. C. Maurya, Int. J. Geom. Methods Mod. Phys. **15**, 1850168 (2018).
[51] S. Capozziello *et al.*, arXiv:1904.01427v1.
[52] J. V. Narlikar, *An Introduction to Cosmology* (Cambridge University Press, Cambridge, England, 2002), p 483.
[53] B. Bertotti, L. Iess, and P. Tortora, Nature (London) **425**, 374 (2003).
[54] A. D. Felice, G. Mangano, P. D. Serpico, and M. Trodden, Phys. Rev. D **74**, 103005 (2006).
[55] Suzuki *et al.*, Astrophys. J. **746**, 85 (2012).
[56] M. Moresco *et al.*, J. Cosmol. Astropart. Phys. 08 (2012) 006.
[57] C. Zhang, H. Zhang, S. Yuan, S. Liu, T.-J. Zhang, and Y.-C. Sun, Res. Astron. Astrophys. **14**, 1221 (2014).
[58] M. Moresco, Mon. Not. R. Astron. Soc. **450**, L16 (2015).
[59] D. Stern, R. Jimenez, L. Verde, M. Kamionkowski, and S. A. Stanford, J. Cosmol. Astropart. Phys. 02 (2010) 008.
[60] V. Sahani, A. Shafieloo, and A. A. Starobinsky, Astrophys. J. Lett. **793**, L40 (2014).
[61] A. G. Riess *et al.* (Spurnova Serach Team Collaboration), Astron. J. **116**, 1009 (1998); Astrophys. J. **607**, 665 (2004); Astrophys. J. **659**, 98 (2007).
[62] P. Astier *et al.*, Astron. Astrophys. **447**, 31 (2006).
[63] T. M. Davis and E. Mörtsell, J. Sollerman *et al.*, Astrophys. J. **666**, 716 (2007).
[64] J. A. S. Lima, J. F. Jesus, R. C. Santos, and M. S. S. Gill, arXiv:1205.4688v2.